Supplementary information

Photo-enhanced Seebeck effect of a highly conductive thermoelectric material

Shizhong Yue, Hanlin Cheng, Hao He, Xin Guan, Qiujian Le, Xinyu Shu, Shu Shi, Jingshen Chen, and Jianyong Ouyang**

The supporting figures

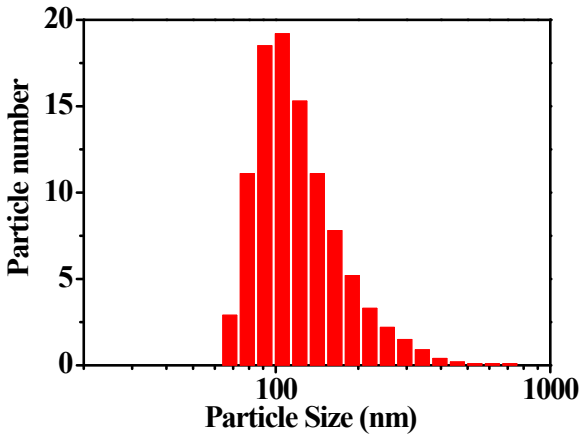

Fig. S1 Dynamic light scattering (DLS). Particle size distribution of an aqueous suspension of TiO_2 nanoparticles.

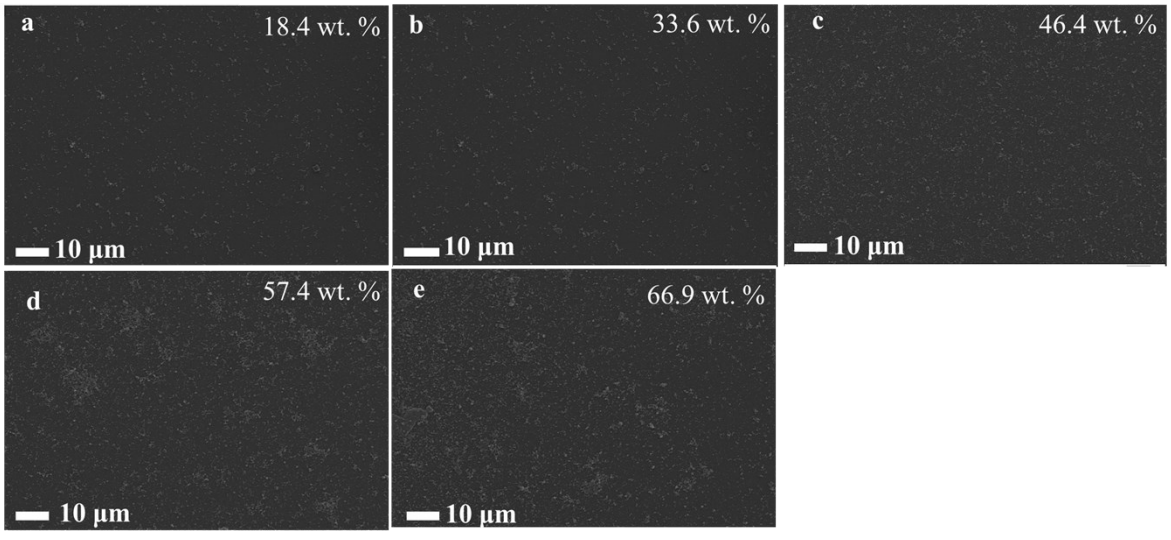

Fig. S2 The SEM image. SEM images of (a) 18.4 wt.%-, (b) 33.6 wt.%-, (c) 46.4 wt.%-, (d) 57.4 wt.%- and (e) 66.9 wt.%-TiO_2@PEDOT:PSS samples.

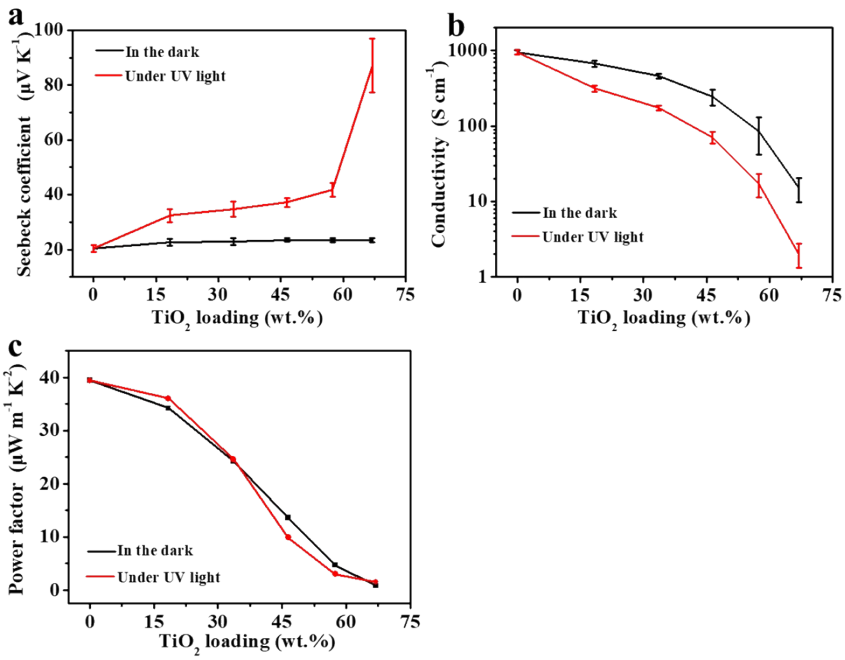

Fig. S3 Thermoelectric properties. Variations of the (a) Seebeck coefficient, (b) conductivity and (c) power factor of the TiO_2@PEDOT:PSS composites in dark and under the UV light with the TiO_2 loading.

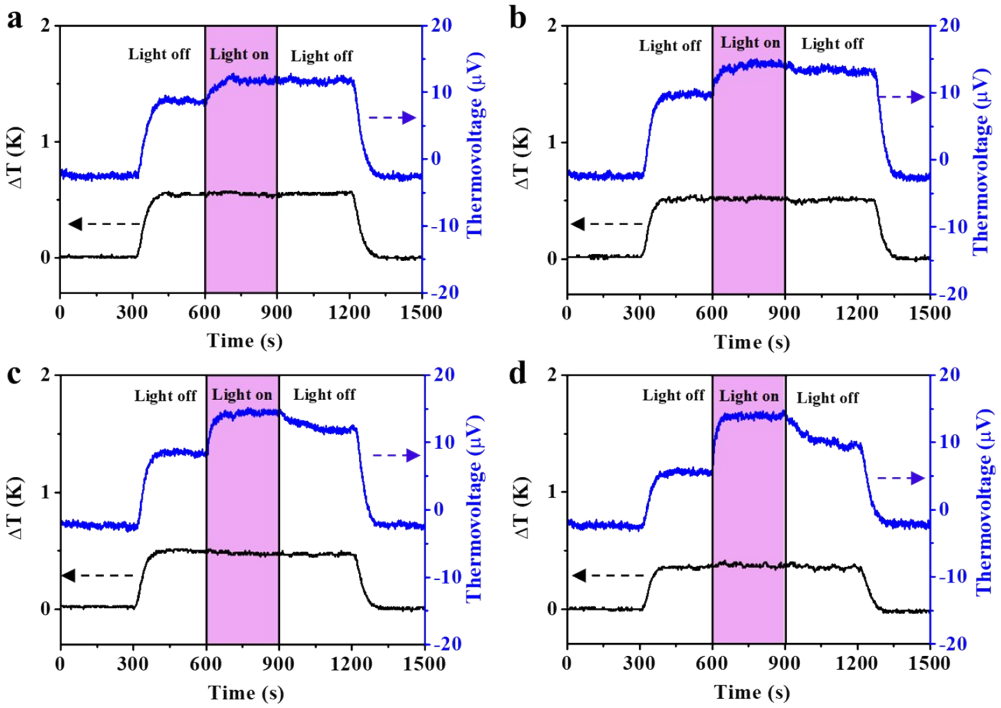

Fig. S4 The thermovoltage changes with the UV light switch. Thermovoltage profiles of (a) 18.4 wt.%-, (b) 33.6 wt.%-, (c) 46.4 wt.%- and (d) 57.4 wt.%-TiO_2@PEDOT:PSS samples when the UV light was turned on and off.

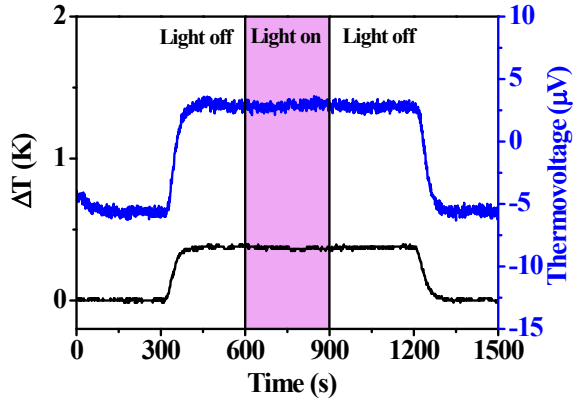

Fig. S5 Thermovoltage profile of a neat PEDOT:PSS sample. No remarkable change was observed when the UV light was turned on and off.

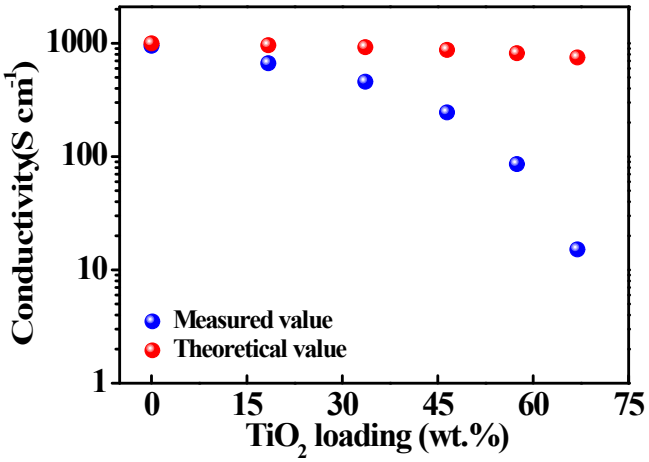

Fig. S6 Variations of the conductivities of TiO_2@PEDOT:PSS composites with the TiO_2. The blue dots are experimental, and the red dots are the simulation results.

.

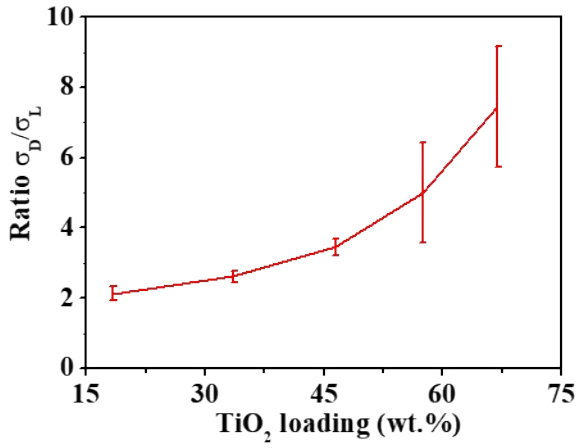

Fig. S7 Variation of the ratio of the conductivity (σ_D) in dark to that (σ_L) under the UV light with the TiO_2 loading.

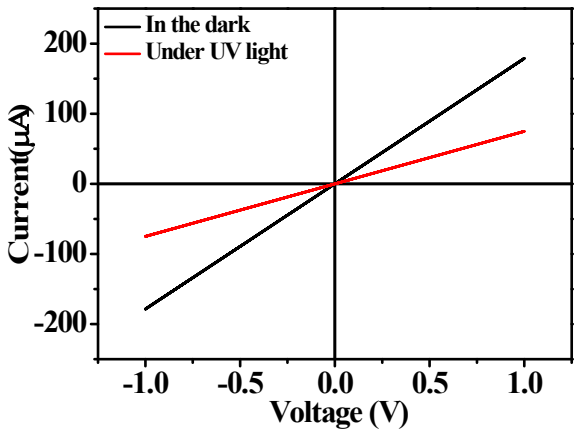

Fig. S8 Current-voltage curves of a device with the structure of (Ag electrode)/33.6%-TiO_2@PEDOT:PSS/(Ag electrode) in dark and under UV illumination.

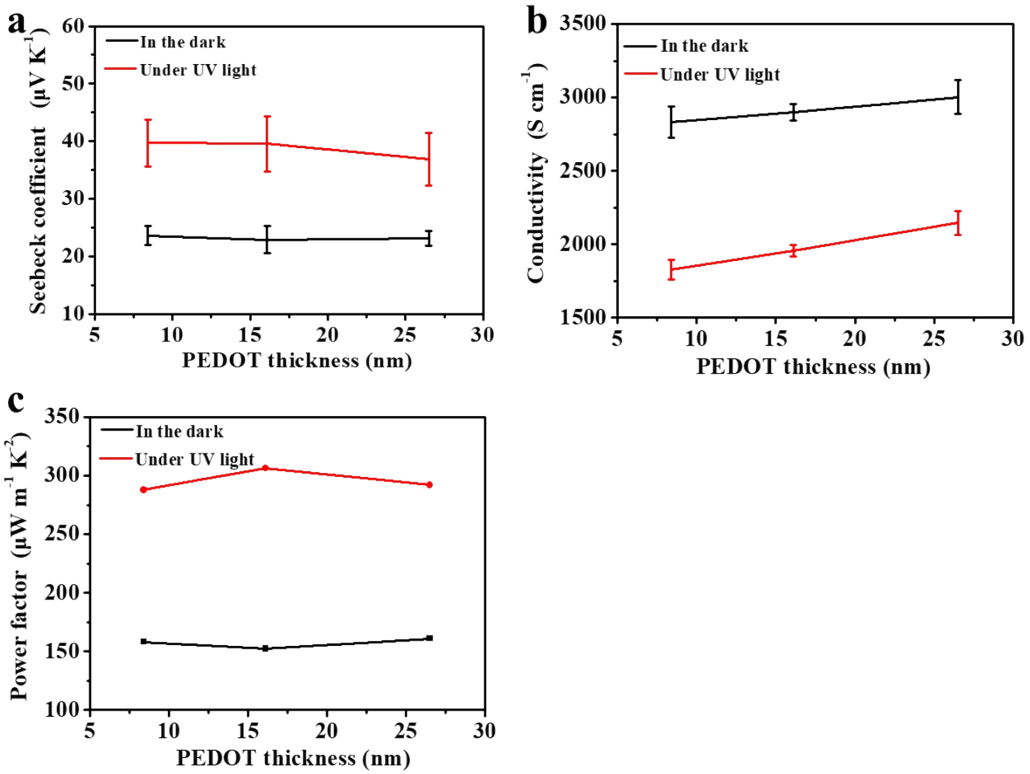

Fig. S9 Thermoelectric properties. Variations of (a) the Seebeck coefficient, (b) conductivity and (c) power factor of TiO_2/PEDOT:PSS double-layer structures in dark or under UV light with the thickness of the PEDOT:PSS layer.

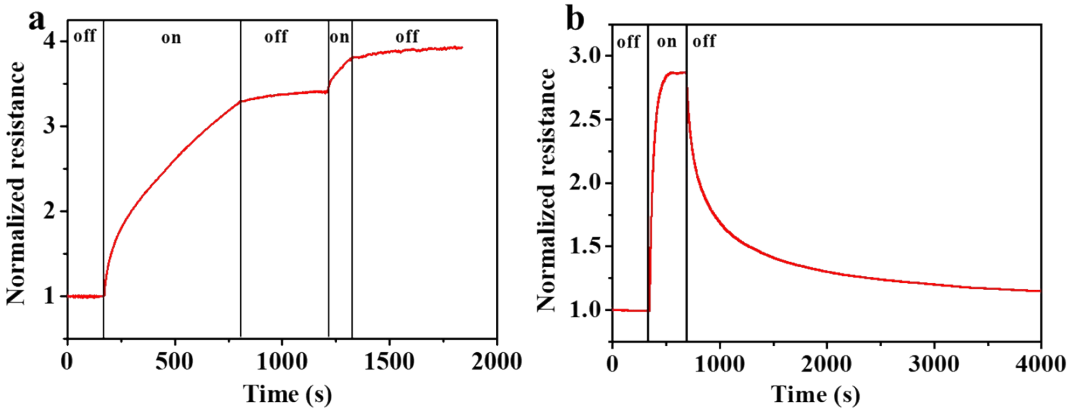

Fig. S10 The resistance evolutions of 33.6%-TiO_2@PEDOT:PSS samples. (a) in N_2 and (b) in air. "On" and "Off" indicate the turning on and off of the UV light, respectively.

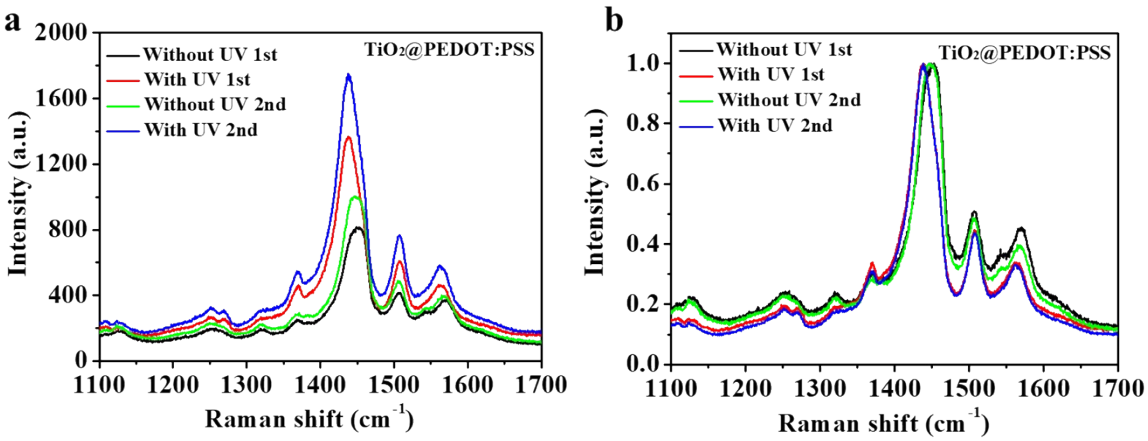

Fig. S11 The Raman spectra. (a) Raman spectra and (b) normalized Raman spectra of 33.6%-TiO_2@PEDOT:PSS samples. The black and red curves are the spectra for the sample before and after the first UV illumination. The sample was then store in air for 2 h, and green and blue curves are the spectra for the sample before and the after the second UV illumination.

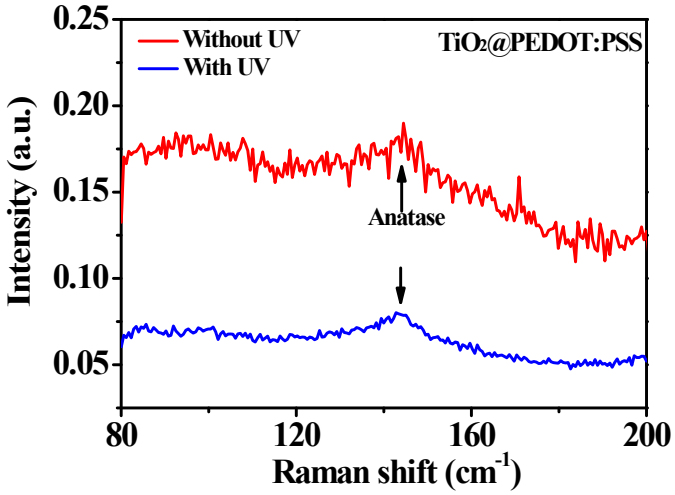

Fig. S12 Raman spectra of a 33.6%-TiO_2@PEDOT:PSS sample without and with UV exposure.

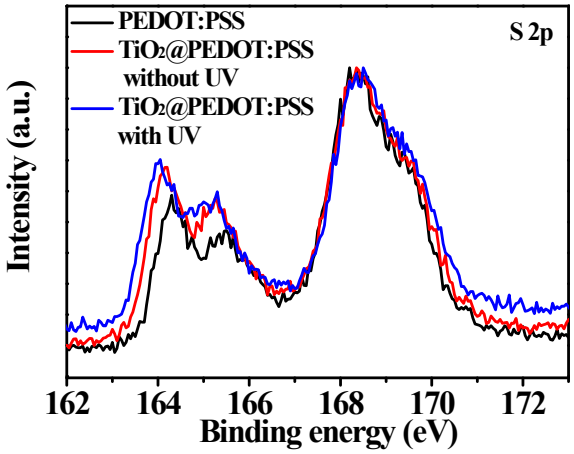

Fig. S13 S2p XPS spectra of neat PEDOT:PSS, 33.6%-TiO_2@PEDOT:PSS without and with the UV exposure.

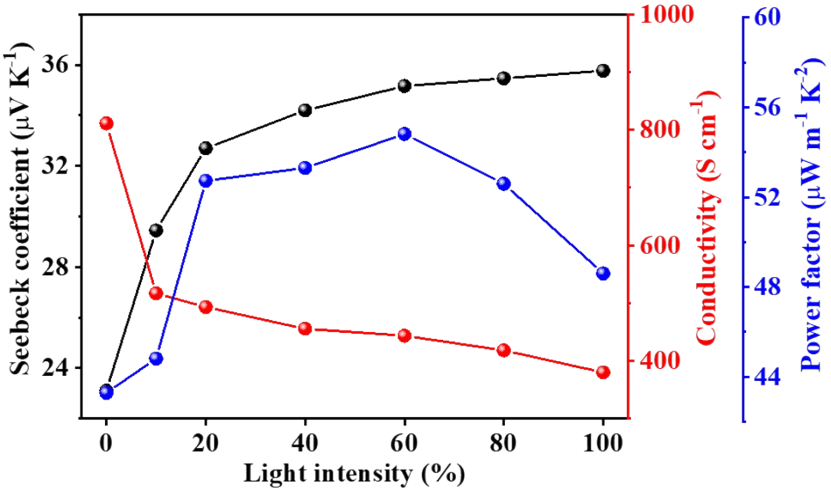

Fig. S14 Thermoelectric properties. Dependences of the thermoelectric properties of a 18.4%-TiO_2@PEDOT:PSS sample with the UV light intensity. The intensity of the UV lamp was controlled by using optical filters.

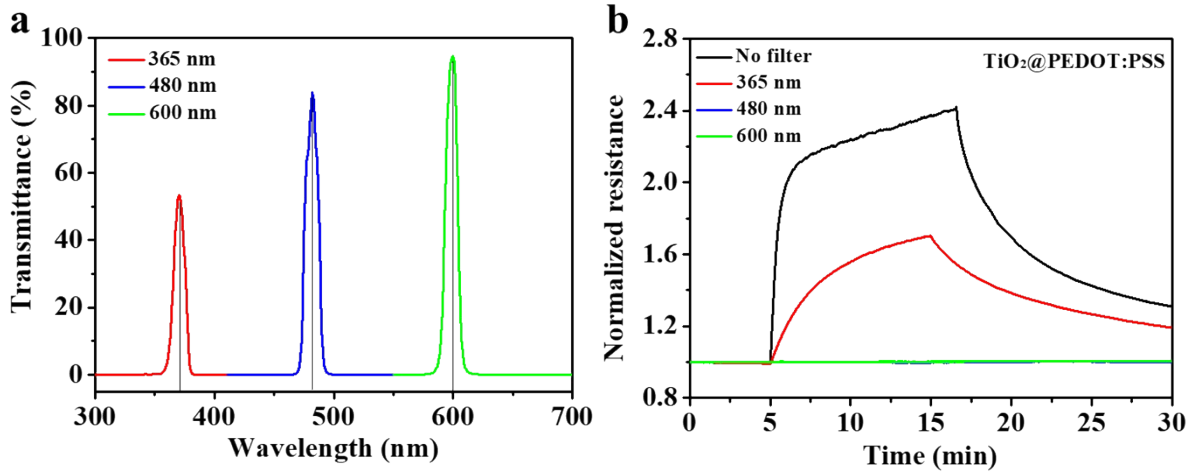

Fig. S15 The resistance changes under different optical filters. (a) The transmittance spectra of three narrow-band optical filters. (b) Resistance evolutions of a 33.6%-TiO_2@PEDOT:PSS sample exposed to light through the three narrow-band optical filters. The solar simulator (AM 1.5) was turned on at 5 min to illuminate the sample. The black curve is the resistance of the sample exposed to unfiltered sunlight, and the red, blue and green curves are for the resistances of the sample exposed to the lights filtered with the 365 nm, 480 nm and 600 nm optical filters, respectively.

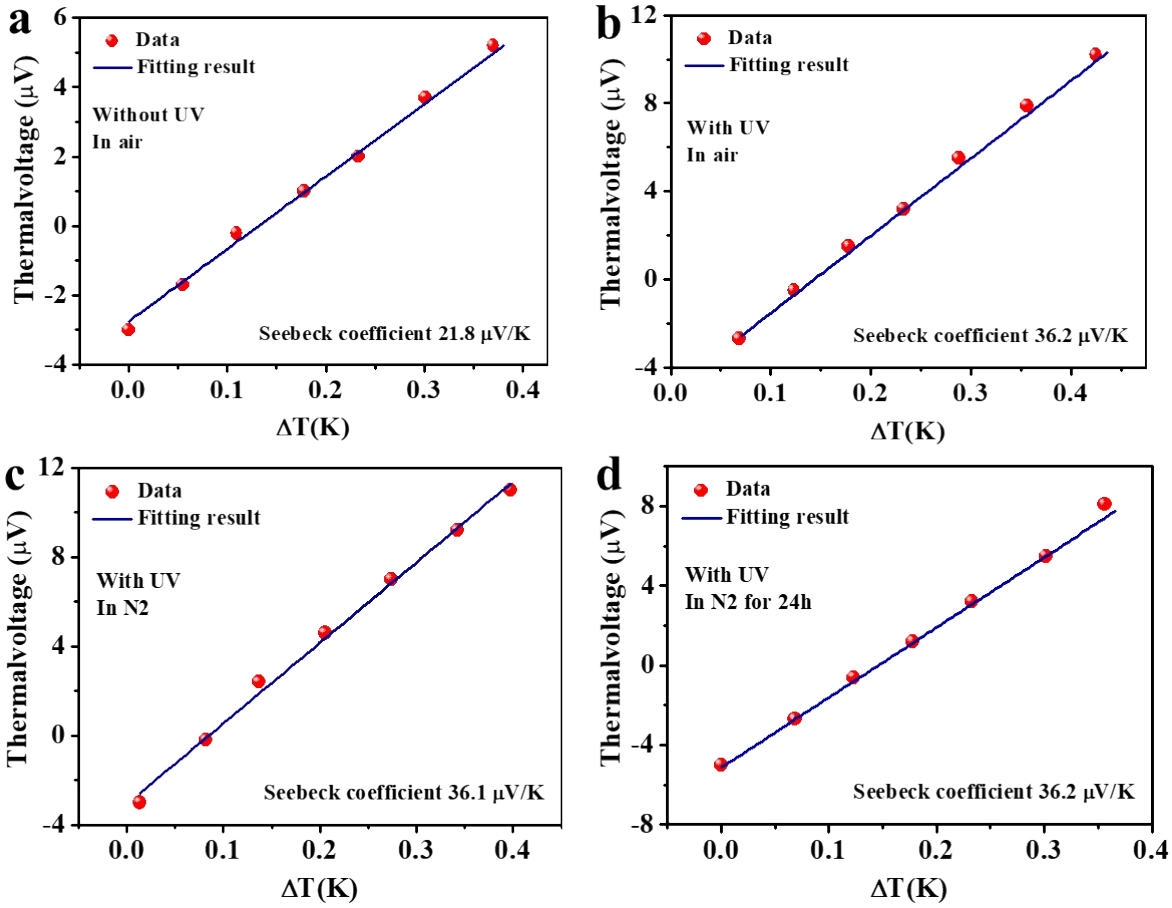

Fig. S16. Testing of the Seebeck coefficient of a sample of 33.6 wt.%-TiO_2@PEDOT:PSS, (a) in air in dark, (b) in air under UV light, (c) immediately after transferred to N_2, and (d) after storage in N_2 for 24 h.